

Evaluation of the Attitude Control System Using Three Dimensional Reaction Wheel for Microsatellites

Yoji Shirasawa(Tokyo Univ.), Atsushi Iwakura,(CDAJ), Yuichi Tsuda(ISAS/JAXA)

Abstract

This paper presents a novel attitude control device which is called three dimensional reaction wheel (3DRW). 3DRW consists of only one levitated spherical mass which can rotate around arbitrary axes by rotational magnetic field. This leads to the reduction of the weight and volume of the system as compared to existing reaction wheel. Furthermore, this device has no mechanical contact between rotor and stator, so the failure caused by the mechanical contact would be reduced.

In this paper, the results of the analysis and experiment on the dynamics and control of 3DRW are shown. To investigate the dynamics of the rotation mass in a magnetic field without mechanical contact with stator, an air levitation system is used. This makes it possible to control the rotation of mass around arbitrary axes. Furthermore, the characteristic of attitude control using 3DRW is also evaluated, and advantage of 3DRW for very small satellites such as micro-class or nano-class satellite is revealed.

3次元リアクションホイールを用いた宇宙機の姿勢制御システムの解析

白澤洋次 (東京大・院)、岩倉 淳(CDAJ)、津田雄一 (ISAS/JAXA)

摘要

宇宙機の精密な3軸姿勢制御を実現する装置として、リアクションホイールが一般的に用いられている。しかし装置が大型になってしまうため小型の宇宙機に搭載するには適さない。また機械的摺動部を持つために故障を起こす可能性が高い。これらの問題を解決するものとして、3次元リアクションホイールが提案されている。これは、浮上している剛体球に回転磁場を与えることで剛体球内に渦電流を発生させ、それにより得られるローレンツ力を駆動トルクとして剛体球に角運動量を与えるものである。この装置では、機械的摺動部を持たないために耐故障性の向上が見込まれ、また剛体球を3次元的に回転させることで3軸の姿勢制御が可能であり、装置の小型化につながる。

本研究では3次元リアクションホイールを用いた姿勢制御システムについて解析的及び実験的に検討を行った。その結果から制御特性を見積もり、従来のリアクションホイールに対する有用性を比較、検証する。さらに、実際に宇宙機に搭載する上での問題点の検討も行う。

1. Introduction

To realize accurate attitude control, the reaction wheel is commonly used for many satellites. However, it has never used for very small satellite such as micro-class or nano-class satellites. The main reason is that existing reaction wheel is too heavy and take too much space to carry, and also needs too much electricity to work for this class of satellite.

In order for such satellites to have a high precision attitude control capability, a novel attitude control device which is called three dimensional reaction

wheel (3DRW) has been proposed. 3DRW consists of only one levitated spherical mass which can rotate around arbitrary axis, while conventional reaction wheel consists of three or more one-axis rotating mass to realize three axes control as shown in Fig.1. The spherical mass consists of conductive metal, and is rotated by rotational magnetic field. This leads to the reduction of the weight and volume of the system. The spherical mass is kept in a given position by electromagnetic force. This would reduce the failure caused by the mechanical contact. For these reasons, 3DRW has many advantages to conventional reaction wheel.

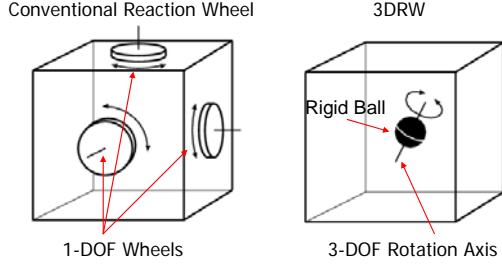


Fig. 1: Conventional reaction wheel and 3DRW

In this paper, the results of the analysis and experiment on the dynamics and control of 3DRW are shown. First, the concept of 3DRW and analytical formulation is introduced. Then, the results of experiment which demonstrates the dynamics of the rotation mass in a magnetic field and the characteristic of open loop control of the rotation. The control system to keep the ball in a given position is also investigated. The results of the experiments are compared with numerical simulations, by which the design method of 3DRW are obtained. Finally, the characteristic of attitude control using 3DRW is evaluated, and it's advantage for microsatellites is revealed.

2. Rotation mechanism of 3DRW

Suppose that a magnetic field is rotating around the rigid ball, and then an eddy current is generated on the surface of the ball. Due to the interference between these magnetic field and eddy current, the Lorentz force is produced on the ball and becomes the rotational torque. The rotational magnetic field can be generated about arbitrary axes; consequently, the rigid ball can be rotated about arbitrary axes.

In this section, the torque of 3DRW generated by magnetic field is investigated.

2-1. Torque Generated by the Rotation Magnetic Field

Fig.2 indicates the analytical model. Suppose that the rigid ball has superior electrical conductivity and rotates in uniform magnetic field. ω is the angular velocity of the ball about z-axis, and \mathbf{B} is intensity of uniform magnetic field.

For the small element on the surface of the ball, let r the vector from the center of the ball to the element, ϕ the angle between x-y plane and the r vector, and θ the angle between x-axis and orthogonal projection of r for x-axis plane.

The voltage induced by the magnetic field in the element is expressed by

$$dV = (\mathbf{v} \times \mathbf{B}) \cdot \mathbf{l} = -r^2 \omega B \cos \theta \cos \phi d\phi \quad (1)$$

where l is the characteristic length of the element. We assume that electric current flows on the surface of the ball along the $\pm z$ direction. Resistance of element is expressed by

$$dR = \frac{l}{\sigma S} = \frac{d(r \sin \phi)}{\sigma \delta \cos \phi r d\theta} = \frac{d\phi}{\sigma \delta d\theta} \quad (2)$$

where σ is the conductivity constant and S is the area of electrical current path in the element, and δ is the effective volume of the element. The electrical current along z-axis is derived as follows:

$$di = \frac{dV}{dR} = -\sigma r^2 \omega B \delta \cos \theta \cos \phi d\theta \quad (3)$$

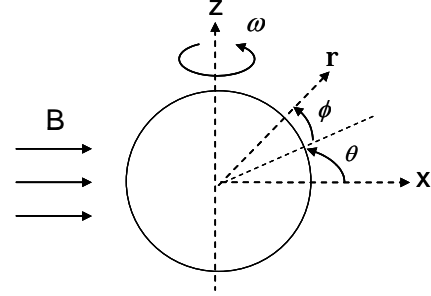


Fig. 2: A schematic diagram of analytical model

Lorentz force is induced on the element by the interaction between the current and the magnetic field as follow:

$$\begin{aligned} dF &= -dl(\mathbf{i} \times \mathbf{B}) \\ &= -\sigma^3 \omega B^2 \delta \cos \theta \cos^2 \phi d\theta d\phi \begin{bmatrix} 0 \\ \cos \phi \\ \sin \phi \sin \theta \end{bmatrix} \end{aligned} \quad (4)$$

By integrating equation (4) for entire surface of the ball, the following equation is derived:

$$T = \int_{-\pi/2}^{\pi/2} \int_0^{2\pi} \mathbf{r} \times d\mathbf{F} d\theta d\phi = -\sigma^4 \omega B^2 \delta \begin{bmatrix} 0 \\ 0 \\ 3/8\pi^2 \end{bmatrix} \quad (5)$$

Assuming that the magnetic field is uniform through the whole sphere for low angular velocity, the torque generated around z-axis is integrated as follows:

$$T = -\frac{3}{40} \pi^2 \sigma^5 \omega B^2 \quad (6)$$

Equation (6) indicates that the torque is generated against the direction of the rotation.

In the actual 3DRW, the ball rotates in inverse direction of the rotating magnetic field. Therefore the rigid ball rotates in the same direction of the rotation magnetic field.

Suppose that the magnetic field rotates relative to the ball, the torque is expressed as

$$T = \frac{3}{40} \pi^2 \sigma^5 (\Omega - \omega) B^2 \quad (7)$$

where Ω is the angular velocity of the rotation magnetic field.

2-2. Torque Generated by Magnet Field Orthogonal to the Rotational Axis

Electric magnets are also used to keep the ball in a given position. If the magnetic field is parallel to the rotational axis of the ball, the disturbance torque would be induced. The torque generated for this

relative position is derived in a similar way to the previous section.

$$T = \int_{-\pi/2}^{\pi/2} \int_0^{2\pi} \mathbf{r} \times d\mathbf{F} d\theta d\phi = -\sigma r^4 \omega B^2 \delta \begin{bmatrix} 0 \\ 0 \\ \pi^2/4 \end{bmatrix} \quad (8)$$

Assuming that the magnetic field is uniform through the whole sphere as before, the torque generated around z-axis is integrated as follows:

$$T = -\frac{1}{20} \pi^2 \sigma r^5 \omega B^2 \quad (9)$$

Equation (9) implies that the torque is generated in a direction opposite to the rotation. Thus, the magnetic field parallel to the rotation axis reduces the spinning rate.

3. Rotation Control System

In this section, the formulation and the results of the experiments of rotation system are shown.

3-1. Equation of Motion

Suppose that the rigid ball rotates at $\boldsymbol{\omega}_{BR} = [\omega_x, \omega_y, \omega_z]^T$ in a coordinate system, Σ_R , remain stationary relative to magnetic field. From the equation (6) and (9), the torque is expressed in the coordinate system as

$$T(t) = -\frac{1}{8} \pi^2 \sigma r^4 \delta \left\{ \begin{bmatrix} 2 & & \\ & 3 & \\ & & 3 \end{bmatrix} B_x(t)^2 + \begin{bmatrix} 3 & & \\ & 2 & \\ & & 3 \end{bmatrix} B_y(t)^2 + \begin{bmatrix} 3 & & \\ & & 2 \end{bmatrix} B_z(t)^2 \right\} \begin{bmatrix} \omega_x \\ \omega_y \\ \omega_z \end{bmatrix} \\ = -\frac{1}{8} \pi^2 \sigma r^4 \delta \left\{ 3B^2 \mathbf{E} + \begin{bmatrix} B_x(t)^2 & & \\ & B_y(t)^2 & \\ & & B_z(t)^2 \end{bmatrix} \right\} \begin{bmatrix} \omega_x \\ \omega_y \\ \omega_z \end{bmatrix} \quad (10)$$

where \mathbf{E} is unit matrix, and B is intensity of magnetic field and satisfies following equation:

$$B = \sqrt{B_x(t)^2 + B_y(t)^2 + B_z(t)^2} = \text{const.} \quad (11)$$

Suppose that Σ_R rotates at Ω relative to the inertial coordinate system and set the coordinate transform matrix from inertial coordinate system to Σ_R , A_{RI} , as

$$A_{RI} = \begin{bmatrix} c\Omega t & -s\Omega t & \\ & 1 & \\ s\Omega t & c\Omega t & \end{bmatrix} \begin{bmatrix} c\theta & s\theta & 0 \\ -c\phi s\theta & c\phi c\theta & s\phi \\ s\phi s\theta & -s\phi c\theta & c\phi \end{bmatrix} \quad (12)$$

where Ωt , ϕ and θ are euler angles of order about z, x then z. Here we set \mathbf{B} as

$$\mathbf{B} = B \left(\cos(\Omega t + \phi) \begin{bmatrix} c\theta \\ s\theta \\ 0 \end{bmatrix} + \sin(\Omega t + \phi) \begin{bmatrix} s\phi s\theta \\ -s\phi c\theta \\ c\phi \end{bmatrix} \right) \quad (13)$$

The angular velocity vector of \mathbf{B} , $\boldsymbol{\omega}_{RI}$, is described as follows:

$$\boldsymbol{\omega}_{RI} = \Omega \begin{bmatrix} -\cos\phi \sin\theta \\ \cos\phi \cos\theta \\ \sin\phi \end{bmatrix} \quad (14)$$

Using

$$\boldsymbol{\omega}_{BR} = \boldsymbol{\omega}_{BI} - \boldsymbol{\omega}_{RI} \quad (15)$$

then equation (10) is transformed as following equation:

$$T = -\frac{1}{8} \pi^2 \sigma r^4 \delta \left\{ 3B^2 \mathbf{E} + \begin{bmatrix} B_x(t)^2 & & \\ & B_y(t)^2 & \\ & & B_z(t)^2 \end{bmatrix} \right\} (\boldsymbol{\omega}_{BI} - \boldsymbol{\omega}_{RI}) \\ = -\frac{1}{8} \pi^2 \sigma r^4 \delta B^2 \mathbf{A}(t) (\boldsymbol{\omega}_{BI} - \boldsymbol{\omega}_{RI}) \quad (16)$$

Assuming that $\mathbf{A}(t)$ is averaged in cycle of rotation, equation (16) is transformed as following equation:

$$T = -\frac{1}{8} \pi^2 \sigma r^4 \delta B^2 \bar{\mathbf{A}} (\boldsymbol{\omega}_{BI} - \boldsymbol{\omega}_{RI}). \quad (17)$$

This equation denotes that we can control the torque by choosing $\boldsymbol{\omega}_{RI}$ properly.

3-2. Experimental Setup

In the experiments, the rotation magnetic field is generated by three or four electrical magnets. A schematic diagram of the rotation system is indicated in Fig.3.

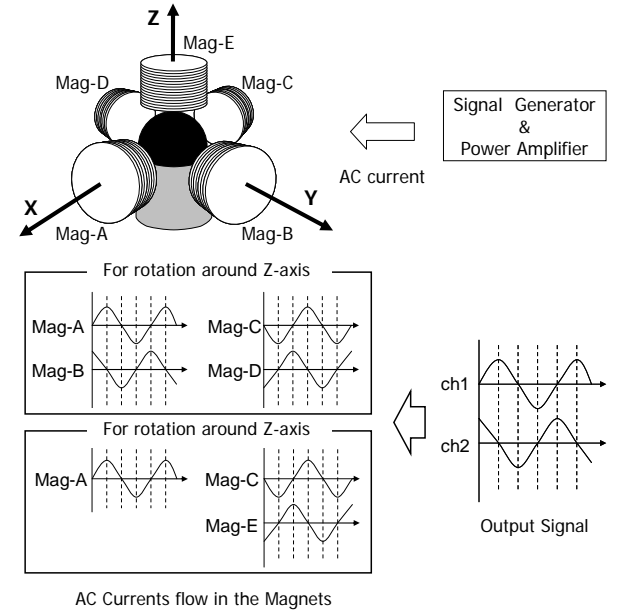


Fig.3: A schematic diagram of the rotation system

The five electrical magnets are positioned around the rigid ball. To rotate the ball around z-axis, mag-A,B,C and D are used. To rotate the ball around x-axis, mag-A,C and E are used. The magnets are applied AC current which is generated by a signal generator and amplified by a power amplifier. To simulate the rotation magnetic field, the AC current has phase difference, $\pi/2$, between adjacent magnets. To investigate the dynamics of the sphere without mechanical contact on the ground, an air levitation system is used. To measure the angular velocity of the ball, laser tachometer is used. The rigid ball is ticked so that the laser tachometer could easily detect the pulse every rotation. Output signal by the tachometer is amplified by operational amplifier circuit, and then logged.

3-3. Experimental Results

In experiments, the frequency of the rotation magnetic field and intensity of it are changed as parameters. The amplitude of signal is the maximum voltage of input signals for power amplifier generated by the signal generator. Frequency of the rotation magnetic field is the same of the signal generated by the signal generator. To observe effects of the intensity and the frequency of the rotation magnetic field, the amplitude of signal and the frequency of the rotation magnetic field are changed.

Fig.4 shows terminal angular velocity in relation to frequency for some input voltage. This denotes that terminal angular velocity of the ball depends on both frequency of the magnetic field and voltage of input signal.

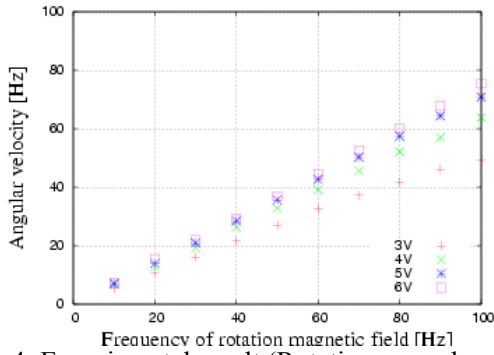


Fig.4: Experimental result (Rotation around z-axis)

Through the experiments, it is found that the angular velocity of the rigid ball can be changed by either the frequency of the rotation magnetic field or intensity of it. Thus if we control the rigid ball same as the conventional reaction wheel, there are 2 ways to control.

3-4. Verification by Numerical Simulation

To verify the formulation of rotation system derived in section 3-1, the numerical simulation is carried out and compared with the results of experiments.

Using equation (7), the rigid ball's equation of rotation as follow:

$$J \frac{d\omega}{dt} = \frac{3}{40} \pi^2 \sigma r^5 B^2 k_e (\Omega(1-s) - \omega) - k_a \omega \quad (18)$$

where J is the inertia moment of the ball, k_e is the efficiency of input torque, s is the slip coefficient, and k_a is the coefficient of the air damper torque proportion to the angular velocity. The values of constant numbers are estimated through some other experiments, and determined as table 1.

Table 1: Determined values of constant number

Constant Number	Determined Value
k_e	0.11
k_a	9.7146×10^{-8} [Nms]
s	0.15

Using these values, the numerical simulations are carried out. Figure 5 shows the results of the simulation about the transient response of angular velocity for 30 and 90Hz, and compared with one of experiments. The results of simulations agree with the one of experiments closely. This denotes that the rotation system is properly expressed by the analytical model of equation (18).

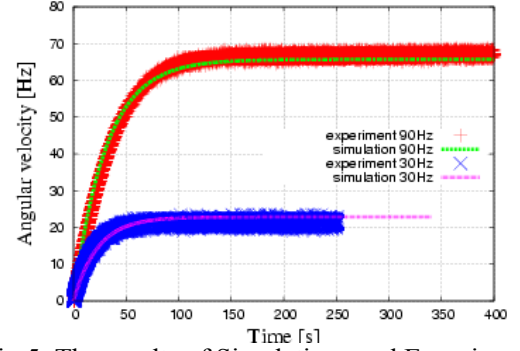


Fig.5: The results of Simulations and Experiments

4. Position control System

To increase the efficiency of the rotation for the lower power consumption, the sphere mass should be set closely to the electromagnets. Therefore, 3DRW needs high accuracy positioning control. This section shows the formulation and experiment of position control system. To keep the sphere mass in a given position, electromagnetic power is used.

4-1. Dynamics and Control

Let x_1 , x_2 , x_3 and u be position relative to the electromagnet, velocity, current and control variable of voltage. Then the model of the system can be expressed as

$$\dot{x}_1 = x_2 \quad (19)$$

$$\dot{x}_2 = -\frac{F_m}{m} + \alpha \quad (20)$$

$$\dot{x}_3 = \frac{R}{L} (k_i u + c_i - x_3) \quad (21)$$

$$F_m = x_3^2 K_{f1} \exp\left(-\frac{x_1}{K_{f2}}\right) \quad (22)$$

where m is weight of the rigid ball. α denotes the acceleration of external force, and sufficiently small compared to the gravity acceleration on the ground. F_m is electromagnetic power, and K_{f1} , K_{f2} are constant numbers which determine the efficiency of electromagnet. Equation (21) denotes the equation of current on the AC circuit, and R , L are resistance and inductance of the circuit. These equations can be linearized around a given position (x_{10} , x_{20} , x_{30}) as

$$\begin{bmatrix} \delta \dot{x}_1 \\ \delta \dot{x}_2 \\ \delta \dot{x}_3 \end{bmatrix} = \begin{bmatrix} 0 & 1 & 0 \\ a_{2,1} & 0 & a_{2,3} \\ 0 & 0 & -\frac{R}{L} \end{bmatrix} \begin{bmatrix} \delta x_1 \\ \delta x_2 \\ \delta x_3 \end{bmatrix} + \begin{bmatrix} 0 \\ 0 \\ \frac{R}{L} k_i \end{bmatrix} \delta u \quad (23)$$

where

$$a_{2,1} = \frac{x_{30}^2 K_{f1}}{m K_{f2}^2} \exp\left(\frac{x_{10}}{K_{f2}}\right) \quad (24)$$

$$a_{2,3} = -\frac{2x_{30} K_{f1}}{m K_{f2}^2} \exp\left(\frac{x_{10}}{K_{f2}}\right) \quad (25)$$

From equation (23), the transfer function $G(s)$ from u to x_1 can be derived as follows:

$$G(s) = -\frac{a_{2,3} R k_i}{(s^2 - a_{2,1})(Ls + R)} \quad (26)$$

From equation (30), $a_{2,1}$ is positive so the system is unstable. Here we use PID controller, and set the compensator $C(s)$ as

$$C(s) = K_p \left(1 + \frac{1}{T_I s} + T_D s\right) \quad (27)$$

where K_p , T_D and T_I are constant gain. The closed loop transfer function $T(s)$ can be written as follow:

$$T(s) = \frac{K T_D s^2 + K s + K/T_I}{L s^4 + R s^3 + (K T_D - L a_{2,1}) s^2 + (K - R a_{2,1}) s + K/T_I} \quad (28)$$

where $K = B R k_i K_p$. By choosing K_p , T_D and T_I appropriately, the position control system would be stable and has required response.

4-2. Experimental Setup

The experimental position control system is shown in Fig.6.

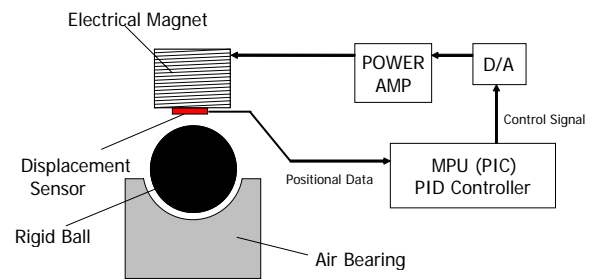


Fig.6: Diagram of the position control system

An electrical magnet is placed over the rigid ball, and a displacement sensor is placed on the magnet. A microprocessor unit receives positional data from the sensor, and controls the current of the electrical magnet through a power amplifier.

To negate gravity acceleration, position control system on the ground needs large electromagnets and electric power. However, actual 3DRW used in space will need few power and small electromagnets for small acceleration.

To simulate the control system under small acceleration, air bearing is used. This allows the ball to move with small power, though this is limited within small range.

The force of the air bearing to levitate the ball decreases in proportion to distance from the equilibrium position. For this case, the external force terms in equation (20) is expressed as

$$\dot{x}_2 = -\frac{F_m}{m} + k_\alpha (x_0 - x_1) \quad (29)$$

where k_α is constant coefficient and x_0 is the the equilibrium position. Correspond to this rewrite, equation (30) is transformed as follows:

$$a_{2,1} = \frac{x_{30}^2 K_{f1}}{m K_{f2}^2} \exp\left(\frac{x_{10}}{K_{f2}}\right) - k_\alpha \quad (30)$$

This denotes that the transfer function $G(s)$ on equation (26) doesn't have the positive pole in case $x_1 > x_0 - F_2$, and the system is stable, while there remains steady state error. This error may vanish by PID controller of equation (27).

To determine the values of constant number used in the previous subsection, some calibration tests are performed. Consequently, the values of constant number are determined as table 3.

Table 3: Constant number on position control system

Constant Number	Determined Value
M	0.1734 [kg]
K_{f1}	0.6374
K_{f2}	2.8031×10^{-3} [m]
R	5.0 [Ω]
L	0.1 [H]
k_α	1.3358×10^4 [s^{-2}]

Using these values, the PID controller's gain are configured and then determined after several trial and error tests. In the experiment, gains are given by $K_p = 0.02$, $T_D = 125$, $T_I = 0.01$.

The simulation result of PID control using above gains are shown in Fig.7. The initial position is $416.5\mu\text{m}$, and the desired position is $11\mu\text{m}$ lower than it. In the transient response, the minimum position is $405.487\mu\text{m}$, so the overshoot is about 0.1% of the displacement. In the stationary response, amplitude of vibration is about 0.01% of it.

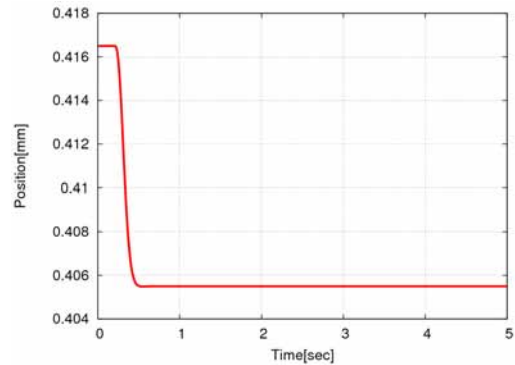


Fig.7: Simulation result of PID control

4-3. Experimental Results

Fig.8 shows the experimental result of PID control of the same condition with simulation. In the transient response, the minimum position is $405.1\mu\text{m}$, so the overshoot is about 4% of the displacement. In the stationary response, amplitude

of vibration is about 5% of it. The electrical current is about 780mA in the transient response and about 50mA in the stationary one. This denotes that very small electrical power is needed to keep the ball in a given position with high accuracy, compared to magnetic levitation systems.

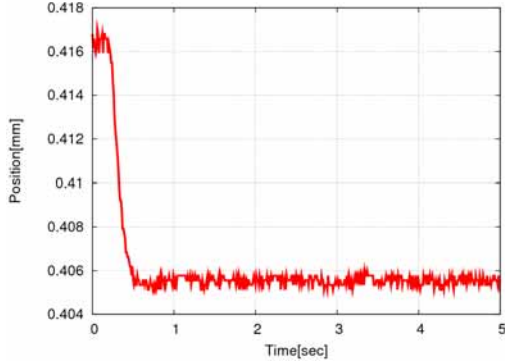


Fig.8: Experiment result of PID control

5. The characteristic of 3DRW

In this section, the characteristic of attitude control using 3DRW is evaluated, and the advantage of 3DRW to conventional reaction wheel for very small satellites is revealed.

5-1. Maximum torque of 3DRW

Here the maximum torque of 3DRW is estimated. The law of conservation of energy is described as

$$\frac{1}{2}I\omega^2 = P \cdot s \quad (31)$$

where P is the electrical power and s is the time of supplying power. From the derivation of this equation, the torque relative to the electrical power can be written as

$$T = I \frac{d\omega}{dt} = K_e P \quad (32)$$

where K_e is the energy conversion efficiency. Take these parameters as $P = 5W$, $K_e = 1\%$, $\omega = 10Hz$, then $T = 7.96 \times 10^{-4} Nm$. This is sufficient order to eliminate the environmental disturbance torque for small satellites.

5-2. Comparing with Conventional Reaction Wheel

Here we estimate the rotor's mass for 3DRW and conventional cylindrical RW for which the same angular momentum, H , is generated by the same angular velocity, ω . For 3DRW, the radius of rotor is

$$R_{3DRW} = \left(\frac{15H}{8\pi\omega} \right)^{\frac{1}{5}} \quad (33)$$

Meanwhile, the radius of rotor for RW is

$$R_{RW} = 2 \left(\frac{2H}{\pi\omega\epsilon} \right)^{\frac{1}{5}} \quad (34)$$

where ϵ is the aspect ratio of the rotor. From these equations, the weight ratio of rotors for conventional RW to 3DRW is obtained. Fig.9 shows the weight ratio relative to ϵ for both no redundancy case and redundancy case. In the first case, the number of rotor is three for RW and one for 3DRW, and 3DRW has the advantage in the weight for $\epsilon > 0.2$. In the latter case, the number is four for RW and two for 3DRW, and 3DRW has the advantage for $\epsilon > 0.4$. For commonly used RW, ϵ is about 0.2 to 0.4, so 3DRW has the advantage for the non redundant system. For the redundant system, 3DRW has the disadvantage in weight. However, the redundancy is 2 for 3DRW and 4/3 for RW, so 3DRW has the advantage in redundancy.

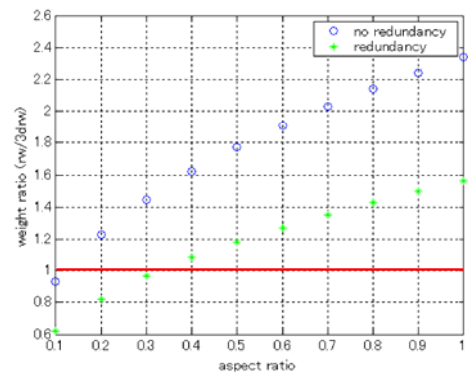


Fig.9: Weight ratio of traditional RW to 3DRW

6. Conclusion

In this paper, the novel attitude control device, 3DRW, is investigated.

The basic dynamic response of the rigid ball is obtained using air bearing. The rigid ball's behavior is dominated by the intensity and the frequency of the rotating magnetic field.

The analytical model of torque and rotation magnetic field is constructed. The results of simulations using analytical model is agree with the results of experiments. Thus the analytical model can be used for practical control.

The position control is also formulated and investigated through the experiments. The ball is controlled with very high accuracy and low electrical current.

Finally, the characteristic of attitude control using 3DRW is evaluated, and the advantage of 3DRW to conventional reaction wheel for very small satellites such as micro-class or nano-class satellite.

7. References

- [1] Atsushi Iwakura, Shinichi Tsuda, Yuichi Tsuda, "The Investigation of 3 Dimensional Reaction Wheel", The 57th International Astronautical Congress(IAC), IAC-06-B5.6.10, 2006.
- [2] Atsushi Iwakura, "The Basic Study of Rotation System using Lorentz force", The 25th International Symposium on Space Technology and Science, Kanazawa, June, 2006.